

# Assessment and Evaluation of Mobilities for Diffusion in the bcc Cr-V-Fe System

Greta Lindwall and Karin Frisk

(Submitted January 9, 2009; in revised form March 25, 2009)

Assessments of diffusion mobility parameters are performed for the bcc Cr-V-Fe alloy system by taking available literature data into account. The main focus is on the diffusion of V in the bcc phase where, in addition to all binaries, ternary interaction parameters are assessed. An experiment is performed in order to study the coarsening of V-rich MC carbide, where the diffusion of V is believed to be of major importance. The measured coarsening rate is compared with the rate calculated using DICTRA, and found to be in satisfactory agreement. The aspects of coarsening experiments as a method to evaluate diffusion mobility data are discussed.

**Keywords** assessment, carbide coarsening, Cr-V-Fe alloys, DICTRA simulation, diffusion mobility database, multicomponent diffusion

## 1. Introduction

Many of the processing steps of tool steels are governed by multicomponent diffusion; for example, segregation and precipitate formation during solidification, spheroidization, or dissolution of the primary precipitates during annealing and austenitizing, and formation and coarsening of secondary precipitates during tempering and services at elevated temperatures. For this reason, knowledge of diffusion characteristics is important in order to improve the properties of a tool steel and to estimate the lifetime of a tool component. In addition, with a tool to predict the evolution of the microstructure, like a diffusion simulator, the time-to-market can be reduced considerably.

One such diffusion simulator is DICTRA.<sup>[1]</sup> This software, as well as many other diffusion simulators, uses coupled thermodynamic data and kinetic data stored in databases. In the last decades a lot of work has been put into the development of thermodynamic databases for many alloy systems, see, e.g., Ref 2. In the case of kinetic databases, the situation is different and, with some exceptions, kinetic data have generally not been systematically assessed yet. One of these exceptions is the work done by Jönsson<sup>[3]</sup> in the early 1990s when he assessed most of the data now included in the MOB1 database.<sup>[1]</sup> Some other assessment works have been performed by Campbell et al.<sup>[4]</sup> and Cui et al.<sup>[5]</sup> Both of these groups' works concern Ni base alloys and diffusion in the fcc

phase. For diffusion in the bcc phase even fewer systems have been assessed. In the work by Jönsson,<sup>[3]</sup> data for diffusion of Cr, Fe, and Ni in a bcc Cr-Fe-Ni alloy were assessed but the bcc Fe-Cr-V alloy system has not yet been fully investigated.

The aim of the work reported here is to assess diffusion data for the lacking system parameters in the case of diffusion in the bcc Fe-Cr-V alloy system. Kinetic data found in literature have been accounted for in the assessments, and control simulations with DICTRA have been performed. Further, a coarsening experiment has been carried out and is compared with simulations where the coarsening model in DICTRA has been utilized.

## 2. Modeling

For a multicomponent system with  $n$  components where the  $n$ :th component is taken to be the dependent one, the Fick-Onsager equation is given by

$$J_k = \sum_{j=1}^{n-1} D_{kj} \frac{\partial c_j}{\partial z}, \quad (\text{Eq 1})$$

where  $J_k$  is the flux of the component  $k$  passing through a unit area per unit time and  $c_j$  is the concentration of component  $j$ . The diffusion coefficient matrix,  $D_{kj}$ , is a product of two matrices; one consisting only of pure thermodynamic information and one consisting of the so-called diffusion mobilities,  $M_B$ ; i.e.

$$D_{kj} \propto M_B \frac{\partial^2 G}{\partial c^2}. \quad (\text{Eq 2})$$

Andersson and Ågren<sup>[6]</sup> suggested that these atomic mobilities,  $M_B$ , should be modeled and stored in the databases rather than the diffusion coefficients directly. Inspired by the Calphad method, they represented the mobilities of the individual species in a multicomponent solution phase as a function of temperature, pressure, and phase composition.

Greta Lindwall and Karin Frisk, Swerea KIMAB, P.O. Box 55970 SE-10206 Stockholm, Sweden. Contact e-mail: greta.lindwall@swerea.se.

## Section I: Basic and Applied Research

By absolute-reaction theory argumentation, the mobility parameter,  $M_B$ , for an element in a given phase can be divided into a frequency factor,  $M_B^0$ , and an activation energy factor,  $Q_B$ :

$$M_B = M_B^0 \exp\left(\frac{-Q_B}{RT}\right) \frac{1}{RT}, \quad (\text{Eq 3})$$

where  $R$  is the gas constant and  $T$  is the temperature. Generally, both  $M_B^0$  and  $Q_B$  will depend upon temperature, pressure, and composition. In the Calphad approach, the composition dependency is expanded as a Redlich-Kister polynomial, and it is possible to expand the logarithm of the mobility instead of the factor itself<sup>[7]</sup>, i.e.

$$RT \ln(RTM_B) = RT \ln(M_B^0) - Q_B. \quad (\text{Eq 4})$$

In the case of a three-component system ( $i$ ,  $j$ , and  $k$ ), the expansion would look like

$$\Phi_B = \sum_i \sum_j y_i y_j \Phi_B^{ij} + \sum_i \sum_{j>i} \sum_{k>j} y_i y_j y_k \left( \sum_r r \Phi_B^{i,j,k} (y_i - y_j)^r \right), \quad (\text{Eq 5})$$

where  $y_i$  is the site fraction of specie  $i$ , the colons in the indices separate the different sublattices and the commas separate different specimens interacting with each other on a certain sublattice.

The temperature dependency of diffusion data, for most phases, may be accounted for by an Arrhenius type of equation. One exception is the effect of ferromagnetic ordering which influences the value of the diffusion coefficient in bcc alloy systems, see, e.g., Ref 8, 9. For systems showing ferromagnetic ordering it is possible to divide the activation energy into two terms,<sup>[10]</sup>

$$Q_B = Q_B^p + \Delta Q_B^{\text{mag}}, \quad (\text{Eq 6})$$

where the first term denotes the activation energy for the mobility in the paramagnetic state and the second term represents the contribution to the activation energy from the magnetic ordering. Different models for the magnetic contribution have been proposed and are reviewed by Jönsson.<sup>[10]</sup> He finds the expression

$$\Delta Q_B^{\text{mag}} = \left[ \alpha_2^{\text{mag}} \Delta H \left( \frac{6}{Q_B^p} - \frac{1}{RT} \right) \right] \quad (\text{Eq 7})$$

to be the most practical for DICTRA. Here  $\alpha_2$  is a factor of proportionality and  $^{\text{mag}}\Delta H$  is the magnetic enthalpy given by the thermodynamic description of the system.<sup>[2,10]</sup> He also finds it reasonable to assume that  $\alpha_2 \neq 0$  for diffusion in bcc alloys, whereas he concludes that the ferromagnetic effect is negligible for fcc alloys; i.e.,  $\alpha_2 = 0$ . In the DICTRA program, a  $\alpha_2$  value of 0.3 is used to account for ferromagnetic ordering for the diffusion of all substitutional elements in the bcc phase. For the interstitial diffusion of carbon and nitrogen, the values  $\alpha_2(\text{C}) = 1.8$  and  $\alpha_2(\text{N}) = 0.6$  are found most suitable to account for the ferromagnetic ordering.<sup>[11]</sup>

## 3. Carbide Coarsening

Once a thermodynamic database and a diffusion mobility database are available, a range of different diffusion phenomena can be simulated with DICTRA. Possible applications are, for example, simulations of coarsening and dissolution of carbides, carbonitrides or nitrides in steels. For this kind of simulation, DICTRA's coarsening model and moving boundary model can be used.<sup>[1]</sup>

The coarsening model in DICTRA uses the approximation that coarsening of a system can be described by carrying out calculations on a particle of maximum size in the center of a spherical cell.

The model obeys the Lifshitz-Slyozov-Wagner (LSW) size distribution of particles; i.e., the maximum particle size is 1.5 times the average particle size.<sup>[12,13]</sup> The so-called interfacial energy,  $\sigma$ , is the driving force for the coarsening and its contribution to the Gibbs energy function is given as

$$\Delta G_m = \frac{2\sigma V_m}{r}, \quad (\text{Eq 8})$$

where  $r$  is the particle radius and  $V_m$  is the molar volume. The simulation is based on local equilibrium at the moving boundary between the maximum particle and the surrounding matrix, taking the interfacial energy contribution into account. Consequently, the value of the interfacial energy has an important influence on the coarsening rate, and since it is one of the inputs needed for the DICTRA simulation, it is a crucial uncertainty for the simulation outcome. In the DICTRA model it is taken to have a constant value, and is, as a rule of thumb, in the range 0.1-1.0 J/m<sup>2</sup>.

## 4. Assessment

From various diffusion experiments, different types of diffusion coefficient data are available; i.e., the tracer or self diffusivity, the intrinsic diffusivity and the chemical diffusivity. This data can be used for the assessment of the database parameters. The tracer diffusivity,  $D_B^* = RTM_B$ , is the most convenient information to use since no thermodynamic factor is needed. Both the intrinsic and the chemical diffusivity depend on the thermodynamic factor and, hence, the assessment of the mobility parameters will depend on the thermodynamic database that is used.

### 4.1 The Fe-V System

In the case of diffusion in the binary bcc Fe-V system, only the self-diffusivity of Fe in bcc Fe has been assessed,<sup>[3]</sup> and assessments of diffusivities of V in bcc V, Fe in bcc V, and the diffusivity of V in bcc Fe remain.

For the self-diffusion of V in bcc V, six different experimental studies have been reported.<sup>[14-19]</sup> In all these works, the <sup>48</sup>V isotope has been studied, except in the work by Günther et al.<sup>[18]</sup> where the <sup>51</sup>V isotope was studied. Single crystals<sup>[14-17,19]</sup> as well as polycrystals<sup>[14,17,18]</sup> were investigated. Putting all these studies together, the vanadium

self-diffusion coefficient has been measured from the temperature 724 to 1642 °C. The temperature dependence of the measured diffusion coefficients (symbols) is shown in Fig. 1 along with calculated diffusion coefficient (solid line) after the assessment. As can be seen, most of the experimental measurements are consistent with one another, except the diffusion coefficient reported by Lundy and McHargue,<sup>[19]</sup> which shows some discrepancy at lower temperatures. In the assessment, this experiment was excluded, whereas all other experimental information were given the same weight.

Geise and Herzig<sup>[20]</sup> studied the impurity diffusion of the <sup>48</sup>V isotope in the paramagnetic state of a bcc Fe alloy, and the work covered a temperature interval from 785 to 899 °C. Since this is the only reported data for impurity diffusion of V in bcc Fe found in literature, the atomic mobility values were assessed to reproduce these data exactly (see Fig. 2).

In the matter of the impurity diffusion of Fe in the bcc V system, four sets of experimental data are to be found.<sup>[14,21-23]</sup> Peart<sup>[14]</sup> studied the <sup>59</sup>Fe isotope in both single crystals and polycrystals in the temperature interval 842-1171 °C. Coleman et al.<sup>[21]</sup> and Neumann and Tölle<sup>[22]</sup> studied the <sup>55</sup>Fe and <sup>58</sup>Fe isotopes in the temperature intervals 960-1345 °C and 1415-1817 °C, respectively. Ablitzer et al.<sup>[23]</sup> reported values of the Fe impurity diffusion coefficient for two temperature ranges; from 1200 to 1550 °C and from 1550 to 1815 °C. Their study concerned the diffusion of <sup>59</sup>Fe and Fe in single crystals and polycrystals. All the experimental data reported are consistent and were given the same weight in the assessment. The temperature dependency of experimental diffusion coefficients (symbols) are

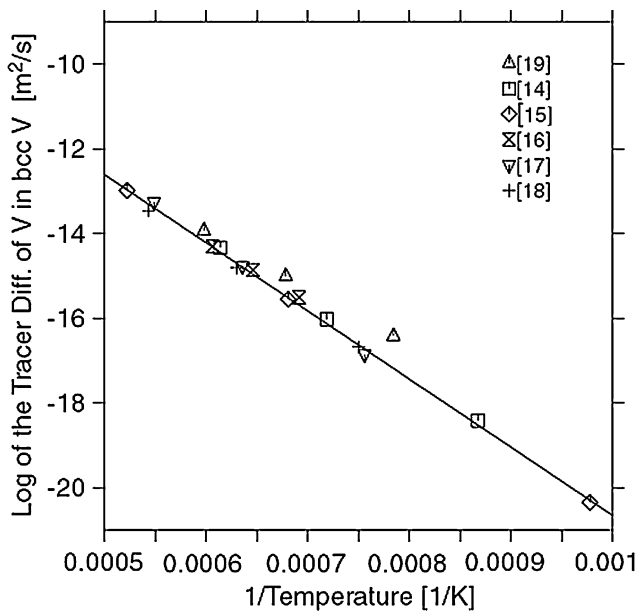


**Fig. 1** The logarithm of the tracer coefficient of V in a bcc V matrix (solid line) as a function of temperature in comparison with measured coefficients (symbols)

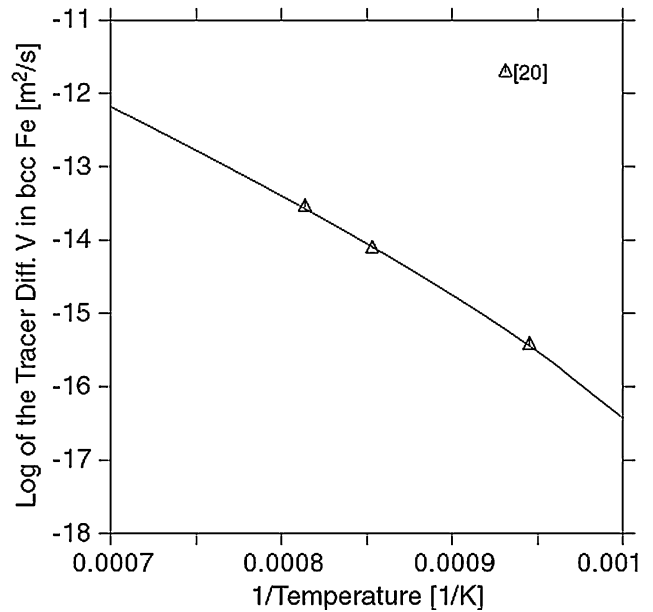


**Fig. 2** The logarithm of the tracer coefficient of V in a bcc Fe matrix (solid line) as a function of temperature in comparison with measured coefficients (symbols)

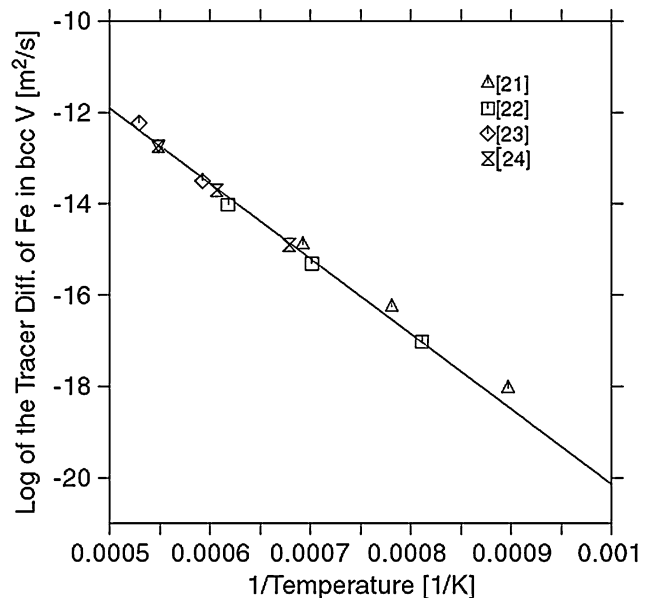


**Fig. 3** The logarithm of the tracer coefficient of Fe in a bcc V matrix (solid line) as a function of temperature in comparison with measured coefficients (symbols)

compared to the calculated diffusion coefficient (solid line) in Fig. 3.

Quantitative assessment results for the bcc Fe-V system are given in Table 1. These values are the parameter values which are implemented in the diffusion mobility database.

Experimental works on diffusion of V and Fe in the bcc Fe-V alloy system have also been reported<sup>[24-27]</sup> and, hence,

**Table 1** Assessment results for the binary Fe-V alloy system

Parameter	Value	Reference
Mobility of V		
MQ(bcc,V:Va;0)	-308051	[15-19]
MF(bcc,V:Va;0)	-87.386·T	
MQ(bcc,Fe:Va;0)	-201974	[14]
MF(bcc,Fe:Va;0)	-89.051·T	
MQ(bcc,V,Fe:Va;0)	74193	[25,27,28]
MF(bcc,V,Fe:Va;0)	0·T	
Mobility of Fe		
MQ(bcc,V:Va;0)	-315361	[21-24]
MF(bcc,V:Va;0)	-70.343·T	
MQ(bcc,Fe:Va;0)	-218000	[3]
MF(bcc,Fe:Va;0)	-83.036·T	
MQ(bcc,V,Fe:Va;0)	112059	[26]
MF(bcc,V,Fe:Va;0)	0·T	

Va = vacancies

it was possible to make conclusions about higher-order Fe-V interaction parameters. One work<sup>[24]</sup> concerned chemical interdiffusion data for diffusion of V in an inhomogeneous Fe-V alloy, whereas the other works concerned tracer diffusion of Fe<sup>[25]</sup> and V<sup>[26,27]</sup> in a homogenous Fe-V alloy. Hanneman et al.<sup>[24]</sup> aimed to study the effect of high pressure on the chemical interdiffusion coefficient, and for this purpose atmospheric and high pressure binary diffusion couples were analyzed by an electron beam microprobe. This gave them concentration versus distance profiles, and the interdiffusion coefficients were determined for various temperatures and pressure conditions by Matano and Hall techniques. The reported diffusion data cover a concentration range up to 30 at.% V and a temperature interval from 950 up to 1250 °C. No pressure dependency is accounted for in the current work, and therefore only the atmospheric interdiffusion data were included in the assessment. Lai and Borg<sup>[25]</sup> studied the tracer diffusion of <sup>59</sup>Fe for Fe-V alloy systems with two different V contents; one with 1.8 at.% V for temperatures from 900 to 1500 °C and one with 5.3 at.% V for temperatures from 900 to 1193 °C. The tracer diffusion coefficients for diffusion of V in the Fe-V alloys systems were experimentally determined using the <sup>48</sup>V isotope by Bowen and Leak<sup>[26]</sup> and Obrtlík and Kucera.<sup>[27]</sup>

Bowen and co-workers investigated a V concentration interval up to 20 wt.% V covering temperatures from 1000 to 1450 °C. The work by Obrtlík et al. included concentrations up to 90 wt.% V and a temperature interval from 839 to 1320 °C. Both works concluded that the diffusivity of V decreases with increasing V concentrations (see Fig. 4). Further, Obrtlík et al. found a linear concentration dependency of the logarithm of the diffusion coefficient in Fe-V primary solid solutions whereas it is parabolic in the V-Fe solid solutions. They concluded that the transition from linear to parabolic dependency occurs somewhere between 28 at.% and 50 at.% V, and pointed out that more detailed data for this effect were needed.

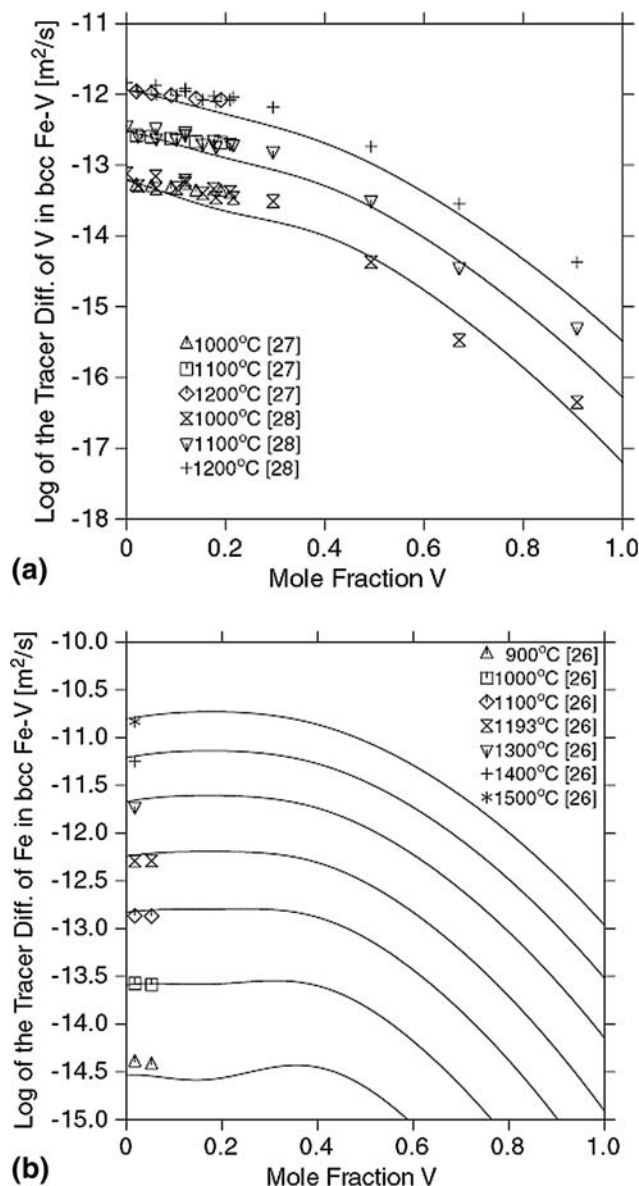


**Fig. 4** The logarithm of the tracer diffusion coefficient of (a) V and (b) Fe in a bcc Fe-V alloy (solid lines) as a function of V concentration for different temperatures in comparison with experimental measurements (symbols)

The assessment results for the mobility interaction parameters are listed in Table 1, and the calculated chemical interdiffusion coefficient and the tracer diffusion coefficients as a function of the V concentration are compared to the measured ones in Fig. 4 and 5. Since the experimental information only included data for limited concentration intervals, calculation results far outside these intervals should be regarded with some caution.

However, consistent with the findings by Obrtlík and Kucera,<sup>[27]</sup> the calculations point to a parabolic concentration dependency of the logarithm of the diffusion coefficient in the case of a V-rich solution (see Fig. 4a). The linear concentration dependency of the calculated diffusion

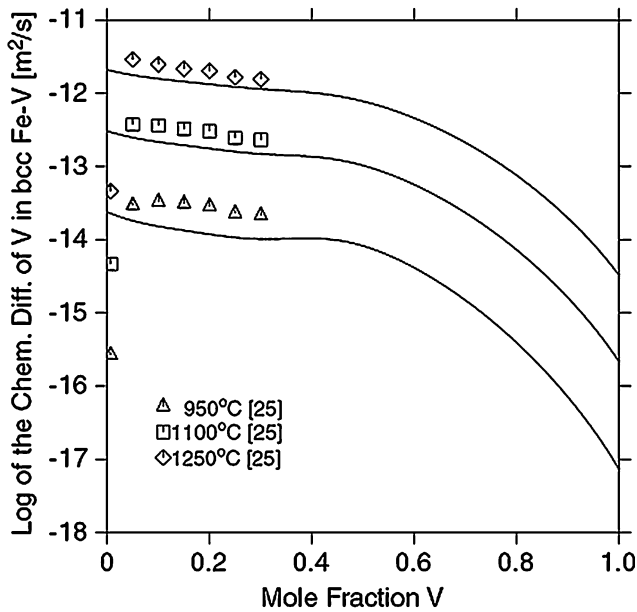


**Fig. 5** The logarithm of the chemical diffusion coefficient of V in a bcc Fe-V alloy (solid lines) as a function of the V concentration for three different temperatures in comparison with experimental measurements (symbols)

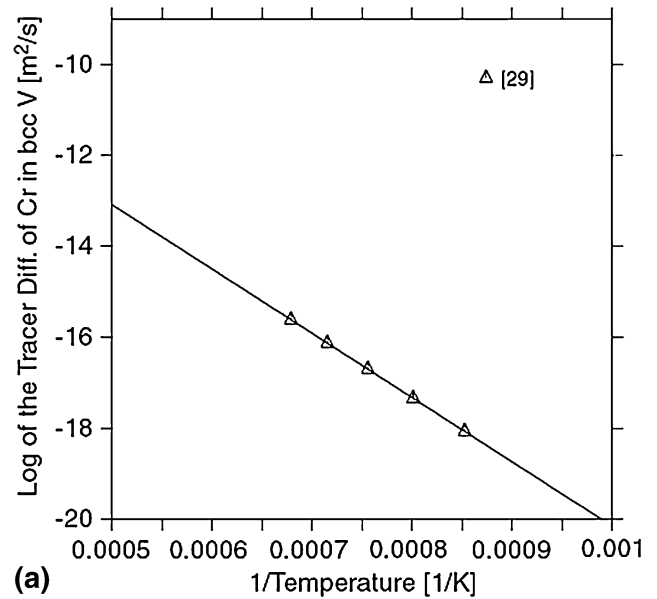
coefficients in the case of a Fe-rich solution is less obvious, and seems to be dependent upon temperature.

#### 4.2 The Cr-Fe-V System

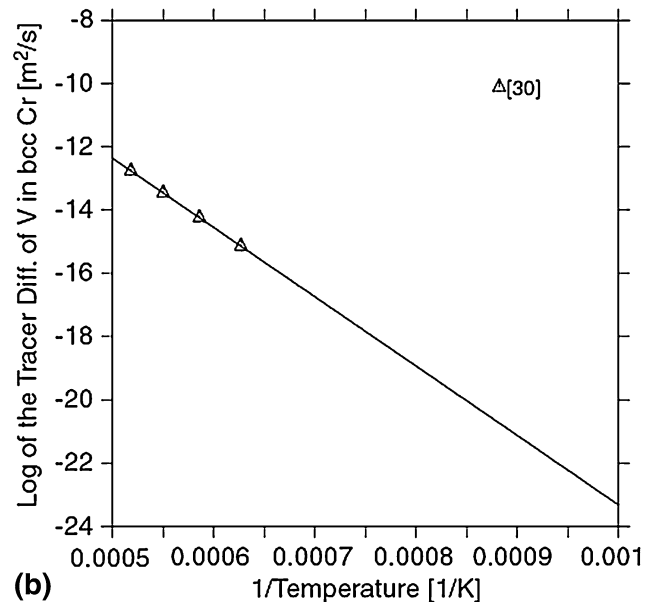
Due to the assessment by Jönsson<sup>[3]</sup> for the diffusion of Cr in bcc Cr, only the mobility parameters for diffusion of Cr in bcc V, and for V in bcc Cr remain to be determined for the binary bcc Cr-V system. For the parameter assessments, two experimental works are to be found; Wolfe and Paxton<sup>[28]</sup> studied the <sup>51</sup>Cr in the case of diffusion in the bcc V system for temperatures ranging from 900 up to 1200 °C using residual activity methods, and Mundy et al.<sup>[29]</sup> studied the <sup>48</sup>V in a bcc Cr system for the temperature interval 1322 to 1768 °C. The diffusion coefficients calculated after the assessments are shown in Fig. 6 (solid lines) in comparison to the measured diffusion coefficients (symbols). The values implemented in the mobility database are listed in Table 2.

The coarsening rate of vanadium carbides in a bcc matrix at elevated temperatures which are in focus in this work is predominately dependent on the diffusion of V. For this reason, the higher order bcc Cr-V-Fe system was also examined, and experimental information for the diffusion of V in the bcc Cr-Fe alloy system at higher temperatures<sup>[30]</sup> as well as lower temperatures<sup>[31]</sup> was used.

Kucera et al.<sup>[30]</sup> measured the diffusion coefficients of V in Fe-Cr alloys with bcc lattice for Cr concentrations up to 26 wt.%. The measurements were carried out in the temperature interval 755 to 1454 °C using the radioisotope <sup>48</sup>V. Extrapolations to temperatures below 627 °C proved to be difficult due to the effect of magnetic ordering on diffusion, and therefore experimental data in this low



(a)



(b)

**Fig. 6** The logarithm of the tracer diffusion coefficient of (a) Cr in a bcc V matrix and (b) V in a bcc Cr matrix (solid lines) as a function of temperature in comparison with experimental measurements (symbols)

temperature region were needed. For this reason, Cermak et al.<sup>[31]</sup> measured the diffusion of V in ferritic Fe-Cr alloys for temperatures from 590 °C up to 830 °C. They investigated the diffusion of the <sup>48</sup>V isotope in three binary ferritic Fe-Cr alloys with 8-12 wt.% Cr, one ternary Fe-12wt.%Cr-0.17wt.%C alloy and two commercial 8 wt.% Cr steels. For the studied alloys they found that the temperature dependency of the diffusion coefficient showed a magnetic anomaly as expected, and that the variation of the Cr content did not influence it. Further, they concluded that the addition of 0.17 wt.% C, or small amounts of other alloying elements, did not significantly affect the coefficient.

**Table 2** Assessment results in the case of the Cr-Fe-V alloy system

Parameter	Value	Reference
Mobility of Cr		
MQ(bcc,Cr:Va;0)	-407000	[3]
MF(bcc,Cr:Va;0)	-35.6·T	
MQ(bcc,Fe:Va;0)	-218000	[3]
MF(bcc,Fe:Va;0)	-77.93·T	
MQ(bcc,V:Va;0)	-270500	[29]
MF(bcc,V:Va;0)	-115.26·T	
Mobility of V		
MQ(bcc,Cr:Va;0)	-418826	[30]
MF(bcc,Cr:Va;0)	-27.246·T	
MQ(bcc,Cr,Fe:Va;0)	262769	[31,32]
MF(bcc,Cr,Fe:Va;0)	-117.559·T	

Va = vacancies

All experimental literature data described above were given the same weight in the assessment, and the assessed results are listed in Table 2. In Fig. 7, the calculated diffusion coefficients (solid lines) as a function of Cr content are shown for three different temperatures, and are compared to the measured ones (symbols). The temperature dependencies for the same coefficients are shown in Fig. 8.

## 5. Coarsening Experiment and Simulation

### 5.1 Experimental

The model alloy was fabricated by casting. Pure chromium (99.99 wt.%), pure vanadium (99.70 wt.%), pure iron (99.98 wt.%), and pure carbon (99.9995 wt.%) were weighed into a total weight of 50 g and placed in an aluminium oxide crucible. The elements were induction heated in a vacuum atmosphere in an electric furnace until melting, and cast in a cold copper crucible into 10 mm diameter bars.

The nominal composition of the alloy was chosen by the help of Thermo-Calc calculations. The goal with the alloy composition was to have an equilibrium situation which consisted of only one carbide phase (MC) in a bcc matrix at the temperature 1150 °C. Another wish was to have a large carbide fraction in order to make measurements easier. The chosen composition fulfilled these requirements as can be seen in Fig. 9, which shows a MC phase fraction of approximately 0.1 at 1150 °C. The analyzed nominal composition of the fabricated model alloy can be seen in Table 3.

A SEM micrograph of the sample microstructure directly after casting is shown in Fig. 10. In order to get to the designed equilibrium situation, and a carbide start size distribution, a sample was first heat treated for 24 h at 1150 °C. Before the heat treatment, the sample was vacuum sealed in quartz capsules to avoid oxidation and loss of elements due to evaporation. A second heat treatment was

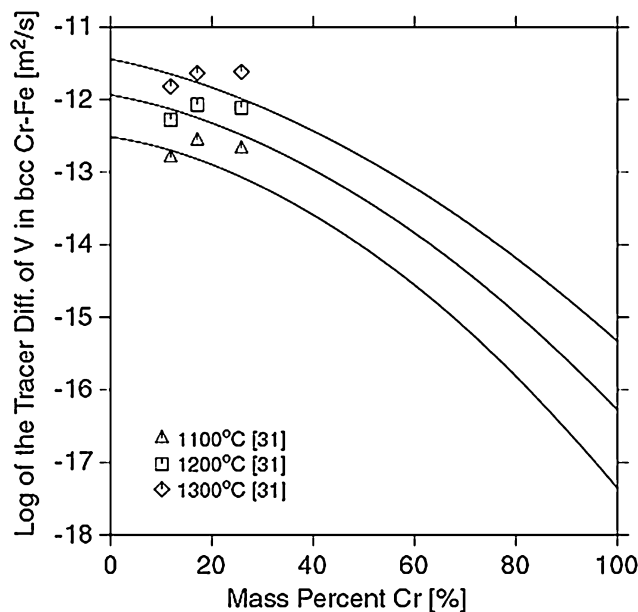


**Fig. 7** The logarithm of the tracer diffusion coefficient of V in a bcc Cr-Fe alloy (solid lines) as a function of the Cr concentration for three different temperatures in comparison with experimental measurements (symbols)

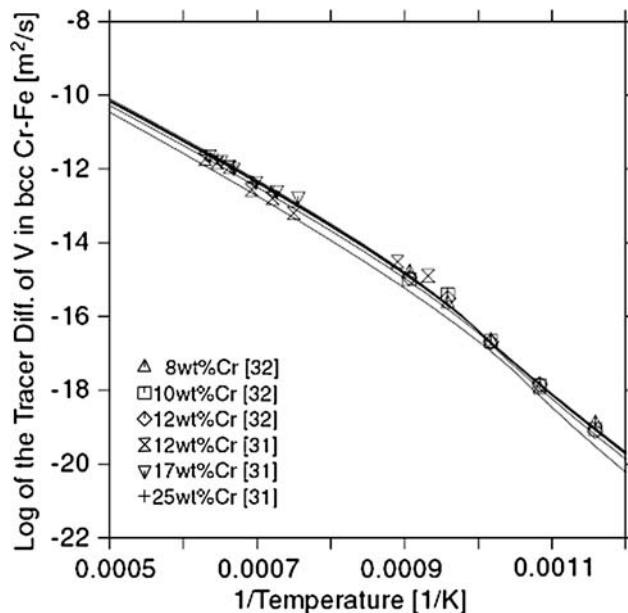


**Fig. 8** The logarithm of the chemical diffusion coefficient of V in a bcc Cr-Fe alloy (solid lines) as a function of temperature for different Cr concentrations in comparison with experimental measurements (symbols)

also performed at 1150 °C for 500 h in order to produce coarsening.

At the end of the heat treatments, the samples were quenched in water, cut in half, and prepared by grinding and polishing to allow for microstructure investigations.

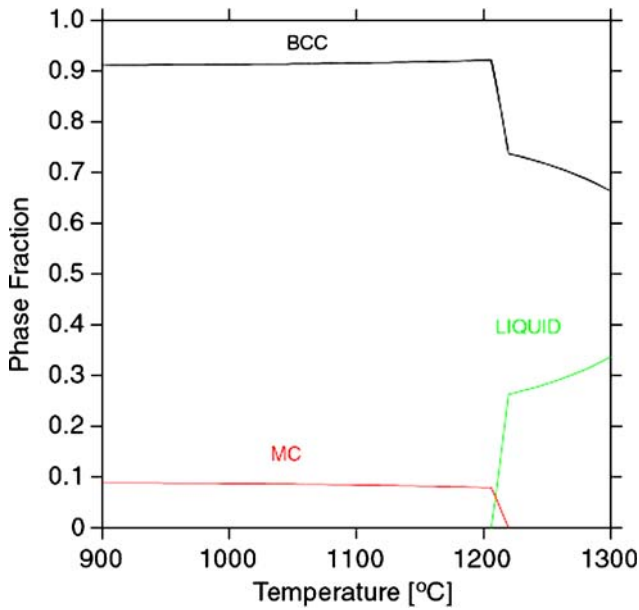


Fig. 9 The phase fractions as a function of temperature for the model alloy composition

Table 3 Analyzed composition in weight percent for the fabricated model alloy

Model alloy	Cr, wt.%	V, wt.%	C, wt.%	Fe, wt.%
A1	17.2	9.2	0.87	Balance

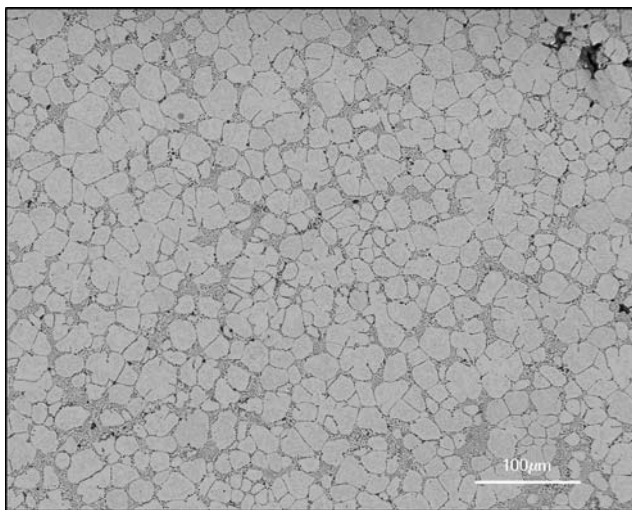


Fig. 10 Microstructure of the model alloy after casting, before heat treatment

The investigations included SEM backscattered electron analysis which gave micrographs for image analysis, EBSD studies in FEG SEM to verify the carbide and matrix phase structure, and EDS/WDS measurements to obtain the composition of the carbides as well as that of the matrix.

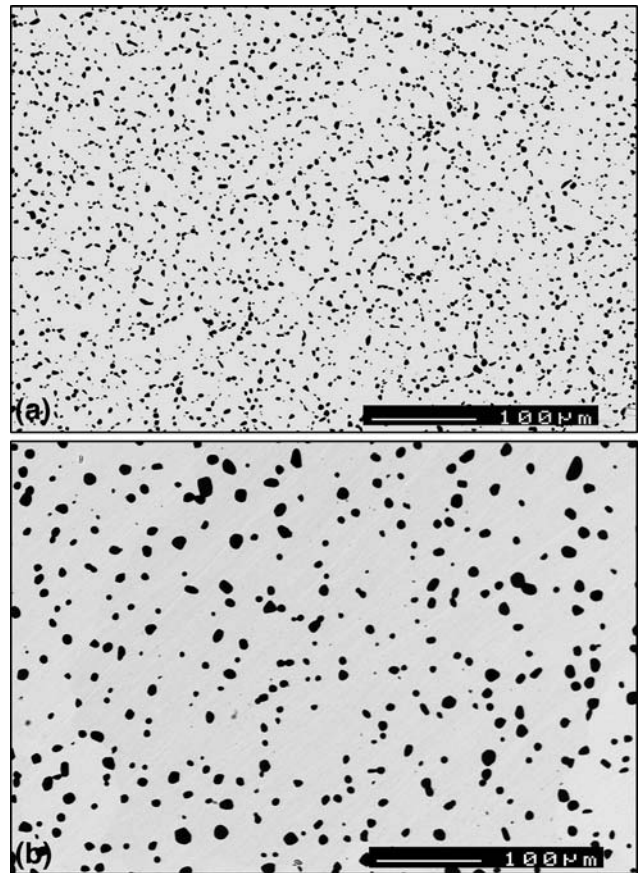


Fig. 11 Microstructure of the model alloy (a) after 24 h of heat treatment at 1150 °C and (b) after 500 h of heat treatment at 1150 °C

For the imaging, a JEOL 7000F and a LEO 15XX electron scanning microscope were used, and for image analysis the MicroGOP software was used; the latter is an apparatus for image processing and quantitative image analysis. Fifteen images (1000×) of each sample were analyzed to obtain the average carbide size distributions. Further, the samples were etched by the Kalling's method No. 1 to reveal information about the sizes of the grains and how these responded to the heat treatment.

Examples of the carbide size distributions for the sample are shown in Fig. 11. The SEM image in Fig. 11(a) shows the distribution after 24 h at 1150 °C at magnification 200 times, and the image in Fig. 11(b) shows the distribution after 500 h at the same temperature. It could be concluded that the carbides are homogeneously distributed throughout the bar, and that their sizes are also relatively equal in different areas of the bar, both for the short time heat-treated sample as well as for the long time heat-treated sample.

The WDS/EDS measurements gave approximately the same carbide and matrix compositions for both heat treatments (see Table 4). This confirms that equilibrium was reached after 24 h of heat treatment and, hence, this carbide size distribution would do as a start condition for the coarsening studies. In Table 4, the calculated carbide and

**Table 4** The measured compositions in atomic percent for the matrix and the carbides in comparison with the calculated

Model alloy A1	Carbide composition at 1150 °C			Matrix composition at 1150 °C		
	Calculated, at.%	Measured, at.%		Calculated, at.%	Measured, at.%	
		24 h	500 h		24 h	500 h
C	43.09	42.12	41.96	0.33	2.63	2.41
V	51.34	51.76	51.97	5.84	6.20	5.91
Cr	4.65	5.14	5.21	18.69	17.41	17.34
Fe	0.92	0.98	0.86	75.14	73.76	74.34

**Table 5** The estimated average carbide diameter before and after the long time heat treatment at 1150 °C

Model alloy	Carbide	24 h at 1150 °C		500 h at 1150 °C	
		$D_{max}$ , $\mu\text{m}$	$D_{eq}$ , $\mu\text{m}$	$D_{max}$ , $\mu\text{m}$	$D_{eq}$ , $\mu\text{m}$
A1	MC	$4.00 \pm 0.09$	$3.08 \pm 0.06$	$7.81 \pm 0.39$	$6.44 \pm 0.34$

matrix compositions are also listed. The calculation was performed with Thermo-Calc in connection to the thermodynamic database TOOLX.<sup>[2]</sup> As can be seen, the calculated and measured compositions are in agreement within experimental errors which validate the accuracy of the thermodynamic data.

By the MicroGOP image analysis, two different types of diameter values were obtained; the maximum diameter,  $D_{max}$ , which reproduces the maximum width of a carbide in the micrograph, and the equal diameter,  $D_{eq}$ , which reproduces the diameter if the area fraction of the carbide is assumed to be a circle. In Table 5, the average of both diameter types are listed for both heat treatments.

The size distribution functions were also given by the MicroGOP software, and the frequency of carbides by count as a function of the carbide diameter is shown in Fig. 12; after 24 h at 1150 °C (a) and after 500 h at 1150 °C (b). It should be noted that these data only represent two-dimensional information.

The etching method Kalling's No. 1 colors ferrite, and since the etch liquid is harsher to the grain boundaries, it could be used to reveal the sample's grain boundaries (see Fig. 13 for optical micrographs). It can be concluded that the carbides predominantly are located at grain boundaries, both after 24 h (a) and after 500 h (b) at 1150 °C. Further, it can be concluded that the grains have grown during the heat treatment and, hence, are larger after 500 h than after 24 h.

## 5.2 Simulation

As mentioned, the value of the interfacial energy is crucial for the result of the coarsening simulation. In the work by Bratberg et al.,<sup>[32]</sup> the interfacial energy was evaluated from coarsening experiments by Wey et al.<sup>[33]</sup>

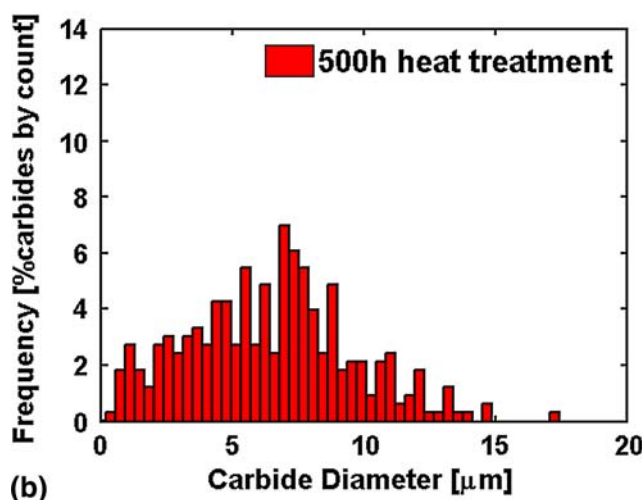
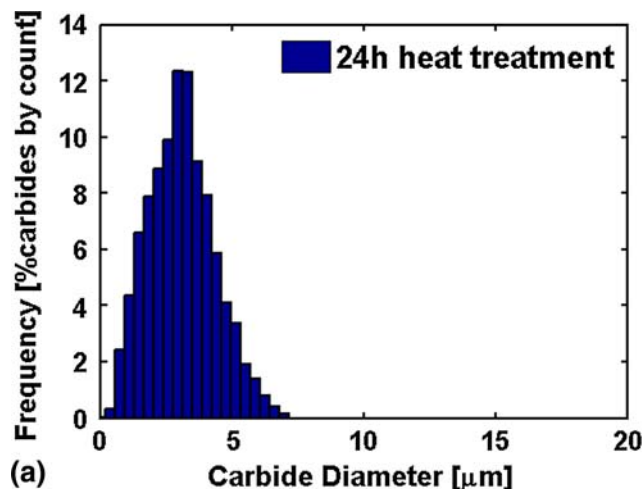


**Fig. 12** The size distribution as a function of particle diameter before the long time heat treatment (a) in comparison with the size distribution after heat treatment (b)

In that work, the coarsening of MC carbides in a fcc matrix was studied and an interfacial energy of  $0.3 \text{ J/m}^2$  in the DICTRA simulation was needed to reproduce their result. This is a reasonable value ( $0.1\text{-}1.0 \text{ J/m}^2$ ) and was therefore used for the simulations in this work.

Other inputs required by DICTRA are the equilibrium composition of the carbide and the matrix, and the initial size of the carbides. These quantities were obtained by Thermo-Calc calculations (equilibrium compositions) and by the diameter measurements described above, see Table 4 and 5.

For the first simulation, the old kinetic mobility database, i.e. the database as it was before the assessments, was used. The simulation result is shown in Fig. 14(a), where the average carbide radius is shown as a function of time. It can be concluded that DICTRA (solid line) overestimates the coarsening rate in comparison to the measured rate (symbols), which is the same conclusion drawn by Bratberg et al.<sup>[32]</sup> for coarsening of a MC carbide in a bcc matrix. For the simulation result after implementation of the new



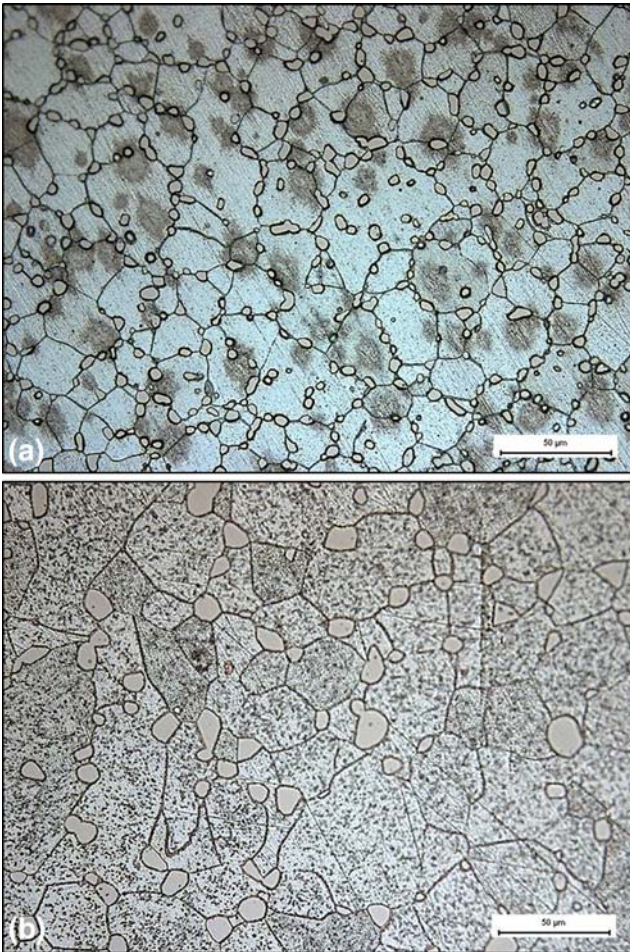


**Fig. 13** The etched microstructure showing the grain sizes (a) before and (b) after the long time heat treatment at 1150 °C

mobility parameters the coarsening rate is lowered (see Fig. 14b) in agreement with experimental findings. For both simulations, the same interfacial energy ( $0.3 \text{ J/m}^2$ ) was used. Figure 14(b) shows also the simulated coarsening rates in the case of the surface energy  $0.1$  and  $0.9 \text{ J/m}^2$ , respectively.

## 6. Discussion

The main conclusion to be drawn from the results presented here is that the simulation outcome strongly depends on the diffusion mobility database that is used and the diffusion data therein. Hence, higher order diffusion data, such as ternary interaction parameters, are decisive for realistic descriptions of the time evolution of the microstructure in multicomponent systems.

Though the results of the data assessment presented in this report lead to good agreement between the DICTRA simulation and the coarsening experiment, it should be noted that the simulation model and the experimental technique used do not come without sources of error.

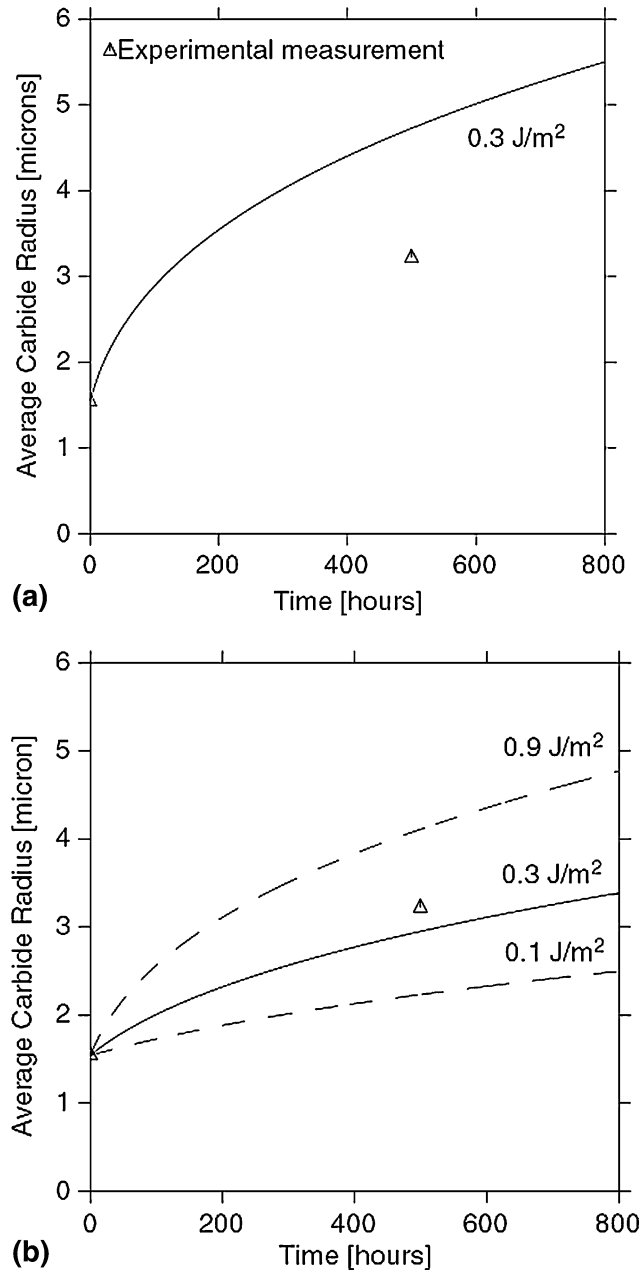


**Fig. 14** The simulated coarsening rate (solid line) for the model alloy carbide in comparison to the measured average carbide size (symbols) before (a) and after (b) the revised kinetic description

One of these sources is the method of producing the model alloy. By casting, the risk of segregation arises, and an uneven composition throughout the sample is possible. However, the heat treatment at high temperature ( $1150 \text{ °C}$ ) facilitates homogenizing, as can be seen by comparison of Fig. 10 with Fig. 11, and if the sample is investigated at approximately the same place before and after the long time heat treatment, the correct change in the microstructure should be observed.

Another source of error is the uncertainty as to the extent of diffusion along high diffusivity paths, such as grain

boundaries. From the micrographs of the etched sample before and after long time heat treatment (Fig. 13), it can be seen that the majority of the carbides are located at the grain boundaries. This cannot be a coincidence and it must be accepted that the grain boundaries and the carbides locations, in one or another way, are correlated.

The LSW model adopted by DICTRA models and calculates the kinetics of coarsening of a spherical particle inside a spherical matrix cell; i.e., volume diffusion of the carbide forming elements in the matrix is the mechanism responsible for the mass transport. Hence, if it is believed that the mass transport, and consequently the coarsening rate for the model alloy carbides studied, is dominated by grain boundary diffusion a comparison with a DICTRA coarsening simulation is irrelevant. On the other hand, if it is believed that the contribution from the grain boundary diffusion is only minor in comparison to the volume diffusion at this high temperature (1150 °C) and that the location of the carbides at the grain boundary is rather an effect of Zener pinning<sup>[34]</sup> of the particles on the boundaries than enhanced grain boundary diffusion, a comparison with the DICTRA coarsening simulation is of interest.

The overview of the microstructure before the long time heat treatment shows an even distribution of carbides over the surface and the carbides have a spherical-like shape. After the long time heat treatment, the carbide shape remains similar to the one observed in the starting microstructure (see Fig. 11), and there is no evidence of preferential coarsening along the grain boundaries. This supports the assumption that the volume diffusion is the rate limiting mechanism. The growth of the grains during the heat treatment can also be explained by the Zener pinning mechanism since the magnitude of the Zener drag force of the carbides on the grain boundaries alternated as smaller carbides dissolve to the benefit for coarsening of larger carbides.

A further uncertainty is the need for specifying a mean scalar value for the surface energy as an input for the DICTRA simulation. Coarsening of carbides is far from a trivial matter, and there are many factors and mechanisms which may influence the coarsening rate. Therefore, assuming that the mass transport is due only to volume diffusion and that the surface energy is a constant scalar value makes the DICTRA coarsening model rather crude. Nevertheless, we believe that this method to evaluate mobility data by coarsening experiments applies as a useful complement to other techniques developed for the extraction of multicomponent diffusion data for systems where ordinary interdiffusion coefficient data normally are not available or difficult to measure. In addition, this method, if used in combination with, for example, diffusion couple experiments, may provide with the possibility to estimate values for the surface energy or to evaluate the area of usage of different simulations.

## 7. Conclusion

This work has included the assessments of parameters describing the diffusion of V and Fe in bcc V, of V and Cr in

bcc V, of V in bcc Cr, of V in bcc Fe-V, and of V in bcc Cr-Fe. This was achieved by accounting for experimental data for diffusion coefficients found in literature. Together with the parameters assessed by Jönsson<sup>[3]</sup> describing diffusion of Cr and Fe in bcc Fe and of Cr and Fe in bcc Cr, all binary interactions in the bcc Cr-V-Fe and two ternary interactions in the case of diffusion in the bcc Fe-Cr-V alloy system are now given a value. The assessed parameters were evaluated by calculating the diffusion coefficients with DICTRA and compared with the experimental coefficients accounted for in the assessments.

This work also included a coarsening experiment where a model alloy consisting of V-rich MC carbides in a bcc matrix was produced and the carbide growth was quantified by investigating the time evolution of the carbide size distribution. A DICTRA coarsening simulation was performed, and the results are in agreement with the experimental findings by using a reasonable value for the surface energy (0.3 J/m<sup>2</sup>).

## Acknowledgments

This work was financed by Böhler Edelstahl, Uddeholm Tooling AB and Böhler-Uddeholm AG. Thanks are dedicated to the research committee; Devrim Caliskanoglu, Ingo Siller and Odd Sandberg, for their interest and support. For the experimental help we wish to thank the colleagues at Swerea KIMAB.

## References

1. A. Borgenstam, A. Engström, L. Höglund, and J. Ågren, DICTRA, a Tool for Simulation of Diffusional Transformations in Alloys, *J. Phase Equilib. Diffus.*, 2000, **21**(3), p 269-280
2. J. Bratberg, Investigation and Modification of Carbide Subsystems in Multicomponent Fe-C-Co-Cr-Mi-Si-V-W System, *Z. Metallkd.*, 2005, **96**(4), p 335-344
3. B. Jönsson, Mobilities in Multicomponent Alloys and Simulation of Diffusional Phase Transformations, Computer Assisted Materials Design (COMMP-93), Sept 6-9, 1993 (Tokyo), p 320-325
4. C.E. Campbell, W.J. Boettinger, and U.R. Kattner, Development of a Diffusion Mobility Database for Ni-Base Superalloys, *Acta Mater.*, 2002, **50**(4), p 775-792
5. Y.W. Cui, M. Jiang, I. Ohnuma, K. Oikawa, R. Kainuma, and K. Ishida, Computational Study of Atomic Mobility for fcc Phase of Co-Fe and Co-Ni Binaries, *J. Phase. Equilib.*, 2008, **29**(29), p 2-10
6. J.O. Andersson and J. Ågren, Models for Numerical Treatments of Multicomponent Diffusion in Simple Phases, *J. Appl. Phys.*, 1992, **72**(4), p 1350-1355
7. B. Jönsson, Assessment of the Mobility of Carbon in fcc C-Cr-Fe-Ni Alloys, *Z. Metallkd.*, 1994, **85**(7), p 502-509
8. J. Fridberg, L.-E. Törndahl, and M. Hillert, Diffusion in Iron, *Jernkont. Ann.*, 1985, **153**, p 263-276
9. A.E. Lord and D.N. Beshers, The Mechanical Damping of Iron from Room Temperature to 400 °C at 400 megacycles/sec, *Acta Metall.*, 1966, **14**(12), p 1659-1672
10. B. Jönsson, On Ferromagnetic Ordering and Lattice Diffusion: A Simple Model, *Z. Metallkd.*, 1992, **83**(5), p 349-355

11. B. Jönsson, Ferromagnetic Ordering and Diffusion of Carbon and Nitrogen in bcc Cr-Fe-Ni Alloys, *Z. Metallkd.*, 1994, **85**(7), p 498-501
12. I.M. Lifshitz and V.V. Slyozov, The Kinetics of Precipitation from Supersaturated Solid Solutions, *J. Phys. Chem. Solids*, 1961, **19**, p 35-50
13. C. Wagner, Theorie der Alterung von Niederschlagen durch Umlosen, *Z. Electrochem.*, 1961, **65**, p 581-591, in German
14. R.F. Peart, Diffusion of V48 and Fe59 in Vanadium, *J. Phys. Chem. Solids*, 1965, **26**(12), p 1853-1861
15. J. Pelleg, Self Diffusion in Vanadium Single Crystals, *Philos. Mag.*, 1974, **29**(2), p 383-393
16. M.P. Macht, G. Froberg, and H. Wever, Selbstdiffusion in Vanadium (Self Diffusion in Vanadium), *Z. Metallkd.*, 1979, **70**(4), p 209-214, in German
17. D. Ablitzer, J.P. Haeussler, and K.V. Sahyrai, Vanadium Self-Diffusion in Pure Vanadium and in Dilute Vanadium-Tantalum Alloys, *Philos. Mag. A*, 1983, **47**(4), p 515-528
18. B. Günther, O. Kanert, and D. Wolf, Nuclear Magnetic Resonance Study of Self-Diffusion in Solid Selenium, *Solid State Commun.*, 1983, **47**(5), p 409-413
19. T.S. Lundy and C.J. McHargue, Diffusion of V48 in Vanadium, *Trans. Metall. Soc. AIME*, 1965, **233**, p 243-244
20. J. Geise and C. Herzig, Impurity Diffusion of Vanadium and Self-Diffusion in Iron, *Z. Metallkd.*, 1987, **78**(4), p 291-294
21. M.G. Coleman, C.A. Wert, and R.F. Peart, Isotope Effect for Diffusion of Iron in Vanadium, *Phys. Rev.*, 1968, **175**(3), p 788-795
22. G. Neumann and V. Tölle, Impurity Diffusion in Body-Centred Cubic Metals: Analysis of Experimental Data, *Z. Metallkd.*, 1991, **82**(10), p 741-744
23. D. Ablitzer, J. Haeussler, K. Sathyraj, and A. Vignes, Diffusion of Iron in Vanadium, *Philos. Mag. A*, 1981, **44**(3), p 589-600
24. R.E. Hanneman, R.E. Ogilvie, and H.C. Gatos, Effect of High Pressure on the Fe-V System Part II: Chemical Interdiffusion, *Trans. Metall. Soc. AIME*, 1965, **233**, p 691-697
25. D.A.F. Lai and R.J. Borg, Diffusion of Iron in Various Ferrous Alloys, US A.E.C., Report: UCRL-50314, 1967
26. A.W. Bowen and G.M. Leak, Diffusion in bcc Iron Base Alloys, *Metall. Trans.*, 1970, **1**, p 2767-2773
27. K. Obrtlík and J. Kucera, Diffusion of Vanadium in the Fe-V System, *Phys. Stat. Sol. (a)*, 1979, **53**, p 589-597
28. A. Wolfe and H.W. Paxton, Diffusion in Bcc Metals, *Trans. Metall. Soc. AIME*, 1964, **230**, p 1426-1432
29. J.N. Mundy, C.W. Tse, and W.D. McFall, Isotope Effect in Chromium Self-Diffusion, *Phys. Rev.*, 1976, **13**(6), p 2349-2357
30. J. Kucera, B. Million, and K. Cihá, Diffusion of Molybdenum, Tungsten and Vanadium in Fe-Cr Alloys with a bcc Lattice, *Kov. Mat.*, 1968, **7**, p 97-107, in Czech
31. J. Cermak, J. Ruzickova, and A. Pokorna, Tracer Diffusion of Vanadium in Fe-Cr Ferritic Alloys, *Scr. Metall. Mater.*, 1995, **33**(7), p 1069-1073
32. J. Bratberg, J. Ågren, and K. Frisk, Diffusion Simulations of MC and M7C3 Carbide Coarsening in bcc and fcc Matrix Utilising a New Thermodynamic and Kinetic Description, *Mater. Sci. Technol.*, 2008, **24**(6), p 695-704
33. M.Y. Wey, T. Sakuma, and T. Nishizawa, Growth of Alloy Carbide Particles in Austenite, *Trans. Jpn. Inst. Met.*, 1981, **22**(10), p 733-742
34. C. Zener, referenced by C.S. Smith, Grains, Phases, Interfaces; An Interpretation of Microstructure, *Trans. AIME*, 1948, **175**, p 15-51